Observation of anisotropic diamagnetism above the superconducting transition in iron pnictide $Ba_{1-x}K_xFe_2As_2$ single crystals due to thermodynamic fluctuations

J. Mosqueira,* J. D. Dancausa, and F. Vidal
Laboratorio de Baixas Temperaturas e Superconductividade (LBTS), Facultade de Física, Universidade de Santiago de Compostela, E-15782 Santiago de Compostela, Spain

S. Salem-Sugui Jr.
Instituto de Fisica, Universidade Federal do Rio de Janeiro, 21941-972 Rio de Janeiro, RJ, Brazil

A. D. Alvarenga
Instituto Nacional de Metrologia Normalização e Qualidade Industrial, 25250-020 Duque de Caxias, RJ, Brazil

H.-Q. Luo, Z.-S. Wang, and H.-H. Wen
National Laboratory for Superconductivity, Institute of Physics and National Laboratory for Condensed Matter Physics, P.O. Box 603, Beijing 100190, People's Republic of China
(Received 21 December 2010; published 15 March 2011)

High-resolution magnetization measurements performed in a high-quality $Ba_{1-x}K_xFe_2As_2$ single crystal allowed to determine the diamagnetism induced above the superconducting transition by thermally activated Cooper pairs. These data, obtained with magnetic fields applied along and transverse to the crystal *ab* layers, demonstrate experimentally that the superconducting transition of iron pnictides may be explained at a phenomenological level in terms of the Gaussian Ginzburg-Landau approach for three-dimensional anisotropic superconductors.

DOI: 10.1103/PhysRevB.83.094519 PACS number(s): 74.25.Ha, 74.40.−n, 74.70.Xa

I. INTRODUCTION

The recent discovery of superconductivity in iron pnictides[1] has generated an intense research activity, in part because they provide an unexpected and very interesting scenario to study the interplay between magnetism and superconductivity.[2] The interest for these compounds is enhanced by the fact that they share many properties with the high-T_c cuprates (HTSC), as the layered structure, a similar evolution of the superconducting parameters with doping, and the proximity to a magnetic transition.[2] As it is still the case of the HTSC, the pairing mechanism in superconducting iron pnictides is not yet known, making the phenomenological descriptions of their superconducting transition a central issue of the present researches on these compounds. As first established in the pioneering experiments by Tinkham and coworkers in low-T_c metallic superconductors,[3] a powerful tool to probe at a phenomenological level the own nature of a superconducting transition is the diamagnetism induced above T_c by thermally activated Cooper pairs.[4] The fluctuation diamagnetism above T_c (sometimes called *precursor diamagnetism*) was also early used to characterize at a phenomenological level the superconducting transition in both optimally-doped[5,6] and underdoped[7] high-T_c cuprates. However, in spite of its interest the precursor diamagnetism received little attention due to both the relative smallness of the superconducting fluctuation effects above T_c in these compounds and, mainly, to the need of high-quality single crystals, with a relatively sharp superconducting transition.[8]

In this paper we report measurements in superconducting iron pnictides of the fluctuation-induced diamagnetism above T_c, which were possible by applying high-resolution magnetometry to a $Ba_{1-x}K_xFe_2As_2$ single crystal with an excellent chemical and structural quality. These data allow an experimental demonstration that the superconducting transition of these materials may be explained at a phenomenological level in terms of the Gaussian Ginzburg-Landau approach for three-dimensional anisotropic superconductors (3D-AGL). This conclusion excludes phase incoherent superconductivity above T_c in iron pnictides, a long standing but still at present debated issue of the HTSC physics.[9,10] Also, it provides a direct check of the fluctuations dimensionality: while bulk low-T_c superconductors (LTSC) behave as three-dimensional (3D) and most HTSC as two-dimensional (2D),[4,6,7] it has been recently proposed that iron pnictides are in an intermediate regime as a consequence of their moderate anisotropy.[11] In relation with this, another interesting aspect of our work is that the fluctuation diamagnetism is probed with magnetic fields applied along the two main crystallographic directions. This allows to accede directly to the superconducting anisotropy factor, but also to study an interesting issue recently observed in other moderately anisotropic superconductor ($NbSe_2$), as it is the anisotropy of nonlocal electrodynamic effects.[12]

II. EXPERIMENTAL DETAILS AND RESULTS

A. Sample fabrication and characterization

The $Ba_{1-x}K_xFe_2As_2$ sample (with $x = 0.28$) used in this work is a $\sim 1.1 \times 0.7 \times 0.1$ mm^3 (430 μg) single crystal. Details of its growth procedure and characterization may be seen in Ref. 13. We have chosen such a small crystal because it presents a well-defined transition temperature which is essential to study critical phenomena. The measurements were performed with a magnetometer based in the superconducting quantum interference (Quantum Design, model MPMS-XL).

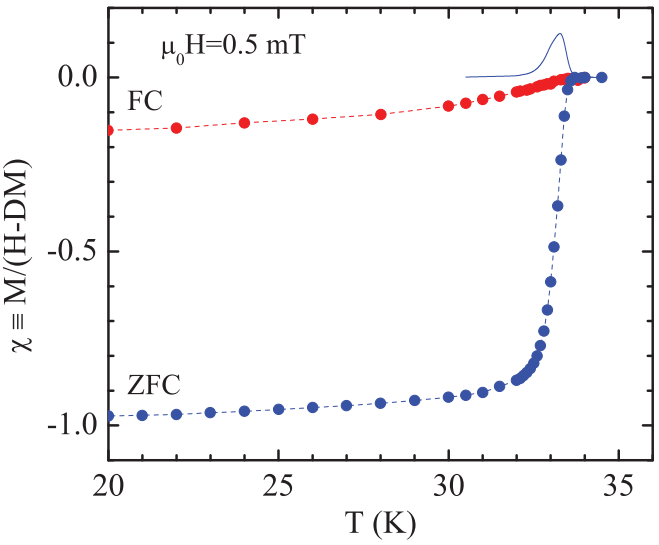

FIG. 1. (Color online) Temperature dependence of the FC and ZFC magnetic susceptibility (already corrected for demagnetizing effects) obtained with a 0.5 mT magnetic field perpendicular to the *ab* layers. T_c and its uncertainty were estimated from the maximum of $d\chi^{ZFC}(T)/dT$ (solid line), and from the high-temperature half-width at half-maximum (this eludes the possible widening associated to the transit through the mixed state).

To position the crystal with the magnetic field, H, applied parallel to the crystal *ab* layers, we used a quartz sample holder (0.3 cm in diameter, 22 cm in length) to which the crystal was glued with GE varnish. Two plastic rods at the sample holder ends ($\sim$ 0.3 mm smaller than the sample space diameter) ensured that its alignment was better than 0.1°. For the measurements with $H \perp ab$ we made a groove ($\sim$ 0.3 mm wide) in the sample holder into which the crystal was glued also with GE varnish. The crystal alignment was checked by optical microscopy to be better than 5°. This allowed to determine the anisotropy factor from the anisotropy of the precursor diamagnetism with a $\sim$ 0.5% uncertainty.[14]

As a first magnetic characterization, in Fig. 1 it is presented the temperature dependence of the zero-field-cooled ZFC and field-cooled FC magnetic susceptibilities, measured with a magnetic field of 0.5 mT perpendicular to the *ab* planes. These measurements were corrected for demagnetizing effects by using as demagnetizing factor $D = 0.78$, which was obtained by approximating the crystal shape by the inscribed ellipsoid. A proof of the adequacy of this procedure is that the ZFC magnetic susceptibility in the Meissner region is close to the ideal value (-1) well below T_c. From these curves we estimated $T_c \approx 33.2 \pm 0.2$ K, which attests the excellent quality of the sample, and allows to study the fluctuation-induced magnetization in almost the whole temperature range above T_c. Such a small transition width is in good agreement with the one determined from the resistive transition of crystals with the same composition and grown following the same procedure.[13]

B. Measurements of the fluctuation diamagnetism around T_c and background subtraction

To measure the effect of superconducting fluctuations above T_c (which according to the 3D-AGL approach, see below, is about 10^{-6}–10^{-7} emu), we used the *reciprocating sample option*. It produces sinusoidal oscillations of the sample about the center of the detection system and improves the resolution by about two orders of magnitude with respect to the conventional DC option. Data were taken by waiting $\sim$ 3 min for complete stabilization after the temperature was within 0.5% the target temperature. For each temperature we averaged six measurements consisting of 15 cycles at 1 Hz frequency. The final resolution in magnetic moment, m, was in the $\sim 10^{-8}$ emu range.

An example of the as measured $m(T)$ data above T_c is presented in Fig. 2(a). As may be clearly seen already in this figure, the $m(T)$ curves present a *rounding* just above T_c (a factor $\sim$ 3 larger in amplitude when $H \perp ab$), which extends few degrees above T_c. In view of the sharp low-field diamagnetic transition (Fig. 1) such a rounding cannot be attributed to T_c inhomogeneities, and is evidence of the presence of an anisotropic precursor diamagnetism in these materials. In the detail around T_c presented in Figs. 2(b) and 2(c), it is clearly seen that the reversible region extends few degrees below T_c, allowing to study the *critical* fluctuation regime, where $m(T)$ presents a similar anisotropy.

The fluctuation-induced contribution was determined from the as measured $m(T)$ by subtracting the *background* magnetic moment, $m_B(T)$, coming from the crystal normal state and in a much lesser extent from the sample holder (this last contribution was estimated to be in the 10^{-6} emu range). Such a background contribution was determined by fitting the function

$$m_B(T) = a + bT + \frac{c}{T} \tag{1}$$

to the raw data in the temperature interval between 37 and 50 K (a, b, and c are free parameters). The lower bound corresponds to a temperature above which the fluctuation-induced magnetic moment is expected to be smaller than the experimental uncertainty (see below). It is worth noting that the use of other plausible functions for $m_B(T)$, for instance $m_B(T) = a + b/(T - c)$, leads to imperceptible changes in the scale of Fig. 2(a).

III. DATA ANALYSIS

A. Theoretical background

In view of the moderate anisotropy observed, the results of Fig. 2 were analyzed in the framework of the 3D-AGL approach. This theory predicts that the fluctuation-induced magnetization for magnetic fields applied perpendicular or parallel to the crystal *ab* layers ($M_\perp$ or $M_\parallel$, respectively) may be obtained from the result for 3D isotropic materials, M_{iso}, through[15–17]

$$M_\perp(H) = \gamma M_{iso}(H) \tag{2}$$

and

$$M_\parallel(H) = M_{iso}\left(\frac{H}{\gamma}\right) = \frac{1}{\gamma} M_\perp\left(\frac{H}{\gamma}\right), \tag{3}$$

where γ is the superconducting anisotropy factor. This transformation was introduced by Klemm and Clem[15] and generalized by Blatter[16] and by Hao and Clem[17] to different

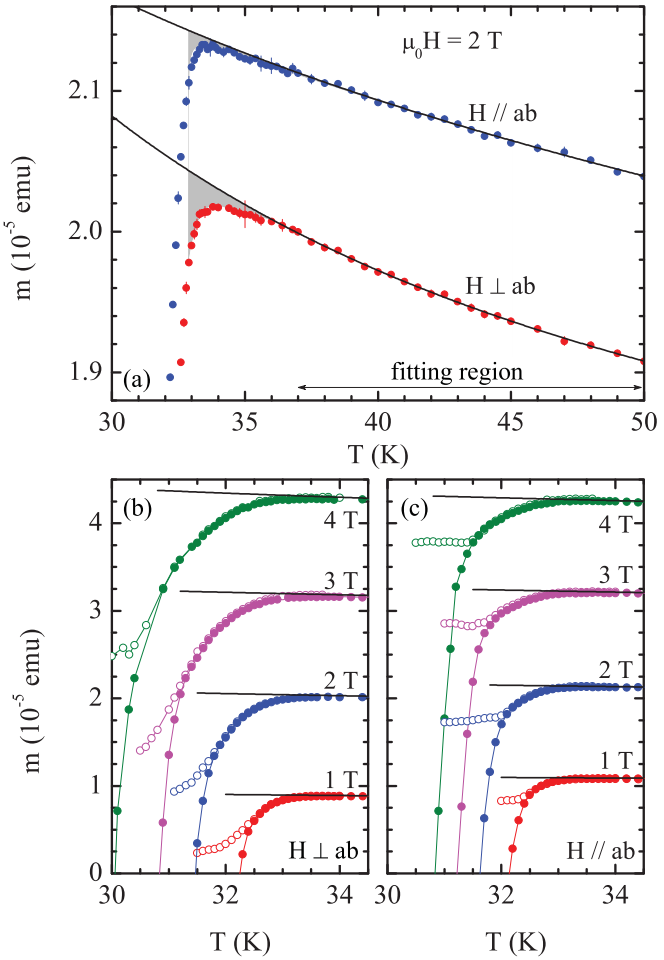

FIG. 2. (Color online) (a) Example of the temperature dependence up to 50 K of the as-measured magnetic moment for a magnetic field applied in the two main crystallographic directions. The normal-state backgrounds (lines) were determined by fitting Eq. (1) in the region indicated. The shaded areas represent the precursor diamagnetism. (b) and (c) Detail around the superconducting transition. Solid (open) symbols were obtained under ZFC (FC) conditions. The diamagnetism above T_c is unobservable in this scale.

observables and different regions in the $H-T$ phase diagram. In particular, it was shown to be also valid for the fluctuation region above T_c.[16] For isotropic materials, the fluctuation magnetization above T_c was calculated in Ref. 18 in the framework of a Gaussian GL approach including a *total-energy* cutoff in the fluctuation spectrum.[19] By combining that result with Eqs. (2) and (3) it follows that

$$M_\perp = -\frac{k_B T \mu_0 H \gamma \xi_{ab}(0)}{3\phi_0^2}\left[\frac{\arctan\sqrt{(c-\varepsilon)/\varepsilon}}{\sqrt{\varepsilon}} - \frac{\arctan\sqrt{(c-\varepsilon)/c}}{\sqrt{c}}\right] \quad (4)$$

and

$$M_\parallel = \frac{M_\perp}{\gamma^2}, \quad (5)$$

where $\varepsilon = \ln(T/T_c)$ is the reduced temperature, $\xi_{ab}(0)$ the *in-plane* coherence length amplitude, $c \approx 0.55$ the cutoff constant,[19] k_B the Boltzmann constant, μ_0 the vacuum magnetic permeability, and ϕ_0 the magnetic flux quantum. These expressions are valid in the low-magnetic field limit, i.e., for $H \ll \varepsilon H_{c2}^{\perp}(0)$ and, respectively, $H \ll \varepsilon H_{c2}^{\parallel}(0) = \varepsilon\gamma H_{c2}^{\perp}(0)$, where $H_{c2}^{\perp}(0) = \phi_0/2\pi\mu_0\xi_{ab}^2(0)$ is the upper critical field for $H \perp ab$ extrapolated linearly to $T = 0$ K. In absence of any cutoff (i.e., when $c \to \infty$) Eq. (4) simplifies to

$$M_\perp = -\frac{\pi k_B T \mu_0 H \gamma \xi_{ab}(0)}{6\phi_0^2}\varepsilon^{-1/2}, \quad (6)$$

which corresponds to the well known Schmidt result.[20]

Equations (4) and (5) predict the vanishing of the precursor diamagnetism at $\varepsilon = c$ (i.e., $T \approx 1.7T_c \approx 56$ K in the present case). This has been experimentally confirmed in a number of HTSC and LTSC,[19] but in the present case the small crystal size does not allow a quantitative check of this onset temperature.[21] The difference between Eq. (4) and the conventional Schmidt approach Eq. (6) is dramatic at high reduced temperatures (typically above $\varepsilon = 0.1$). However, it is still as high as 15% for ε as low as 0.01, which justifies the use of the total energy approach also at low reduced temperatures.

B. Fluctuation diamagnetism in the Gaussian region above T_c

A detail of the fluctuation magnetization above T_c (already corrected for the normal state contribution and normalized by the applied field) is presented in Fig. 3 for both $H \perp ab$ and $H \parallel ab$. In this representation we have only included magnetic fields up to 2 T, which are expected to be in the low-magnetic field regime except in a narrow temperature interval close to T_c. As expected, both $M_\perp/H$ and $M_\parallel/H$ are independent of the applied magnetic field except very close to T_c, where finite-field effects are already observable.[4,18,22] The best fit of Eqs. (4) and (5) to the data in the low-field region is in good agreement with the temperature dependences and amplitudes observed. The values obtained

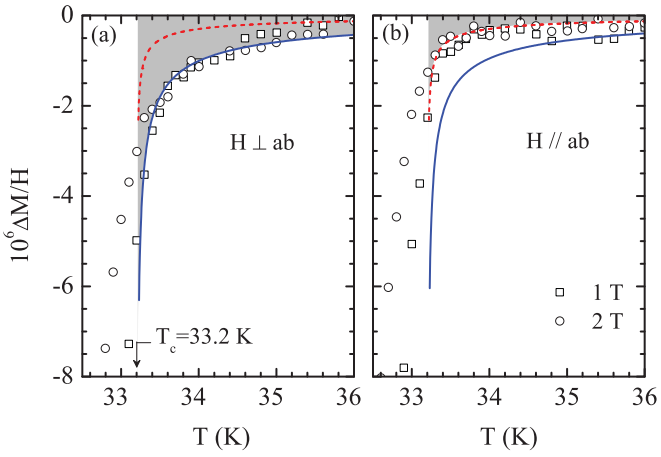

FIG. 3. (Color online) Detail around T_c of the temperature dependence of the fluctuation magnetization (over H) for several magnetic fields applied in the two main crystallographic directions. The lines correspond to the Gaussian 3D-AGL approach in the low magnetic field limit (solid blue for $H \perp ab$ and dashed red for $H \parallel ab$). For a better comparison, both lines are presented in (a) and (b).

for the two free parameters, $\xi_{ab}(0) = 1.5$ nm (which leads to $\mu_0 d H_{c2}^{\perp}/dT = -4.2$ T/K near T_c) and $\gamma = 1.8$, are close to the ones in the literature.[23] These values lead to a *transverse* coherence length $\xi_c(0) = \xi_{ab}(0)/\gamma = 0.83$ nm, larger than the Fe-layers periodicity length (~0.66 nm),[13] which justifies the applicability of the 3D-AGL approach. The $\xi_{ab}(0)$ value is well within the ones in HTSC, and γ is just a few times smaller than in $YBa_2Cu_3O_{7-\delta}$. These similarities contrast with the differences between their precursor diamagnetism (allegedly unconventional in the HTSC).[9] Finally, $\xi_{ab}(0)$ is much shorter than in the moderately anisotropic 2H-$NbSe_2$, which could explain the nonobservation of nonlocal electrodynamic effects when $H \perp ab$ in the present case.[12]

C. Fluctuation diamagnetism in the critical region around T_c

As a check of consistency of the above analysis we studied the data in the critical region, closer to the H-dependent critical temperature, where the fluctuations amplitude is so large that the Gaussian approximation breaks down.[4] This region is bounded by the so-called *Ginzburg criterion*,[24] which according to the transformation to anisotropic materials may be written as

$$T \approx T_c^{\perp}(H) \pm T_c \left[\frac{4\pi k_B \mu_0 H}{\Delta c \xi_c(0) \phi_0}\right]^{2/3} \tag{7}$$

for $H \perp ab$, and

$$T \approx T_c^{\parallel}(H) \pm T_c \left[\frac{4\pi k_B \mu_0 H}{\Delta c \xi_c(0) \gamma \phi_0}\right]^{2/3} \tag{8}$$

for $H \parallel ab$, where Δc is the specific-heat jump at T_c. In this region, the 3D-GL approach in the lowest-Landau-level approximation predicts that $M_{\perp}(T,H)$ follows a scaling behavior, $m_{\perp} = f_{\perp}(t_{\perp})$, the scaling variables being[25]

$$m_{\perp} \equiv \frac{M_{\perp}}{(HT)^{2/3}} \tag{9}$$

and

$$t_{\perp} \equiv \frac{T - T_c^{\perp}(H)}{(HT)^{2/3}}, \tag{10}$$

where $T_c^{\perp}(H) = T_c[1 - H/H_{c2}^{\perp}(0)]$. According to Eq. (3), $M_{\parallel}(T,H)$ should scale as

$$m_{\parallel} = f_{\parallel}(t_{\parallel}) = \frac{f_{\perp}(t_{\parallel}\gamma^{2/3})}{\gamma^{5/3}} \tag{11}$$

the scaling variables being now

$$m_{\parallel} \equiv \frac{M_{\parallel}}{(HT)^{2/3}} \tag{12}$$

and

$$t_{\parallel} \equiv \frac{T - T_c^{\parallel}(H)}{(HT)^{2/3}}, \tag{13}$$

where $T_c^{\parallel}(H) = T_c[1 - H/H_{c2}^{\parallel}(0)]$, and $H_{c2}^{\parallel}(0) = \gamma H_{c2}^{\perp}(0)$.

In Figs. 4(a) and 4(b) the scaling of the $M_{\perp}(T,H)$ and $M_{\parallel}(T,H)$ data according to Eqs. (9), (10), (12), and (13) is presented. For that, $t_{\perp}$ and $t_{\parallel}$ were evaluated by using the $H_{c2}^{\perp}(0)$ and γ values obtained in the analysis of the precursor diamagnetism in the Gaussian region, and $T_c = 33.1$ K (in good agreement with the T_c value resulting from Fig. 1). As may be clearly seen, both scalings are excellent and the relation between the observed scaling functions is in good agreement with Eq. (11). The applicability of the above scalings extends down to the lower bound of the reversible region. This is in agreement with Eqs. (7) and (8), which when evaluated by using $\Delta c/T_c = 0.1$ J/molK^2 (see Ref. 26) and the superconducting parameters resulting from the previous analysis, are in an unexpected agreement with the observed lower bound of the reversible region for both H directions [see Figs. 4(c) and 4(d)]. The 3D scaling was previously found to be adequate when $H \perp ab$,[8] but here its validity is extended to the case in which $H \parallel ab$.

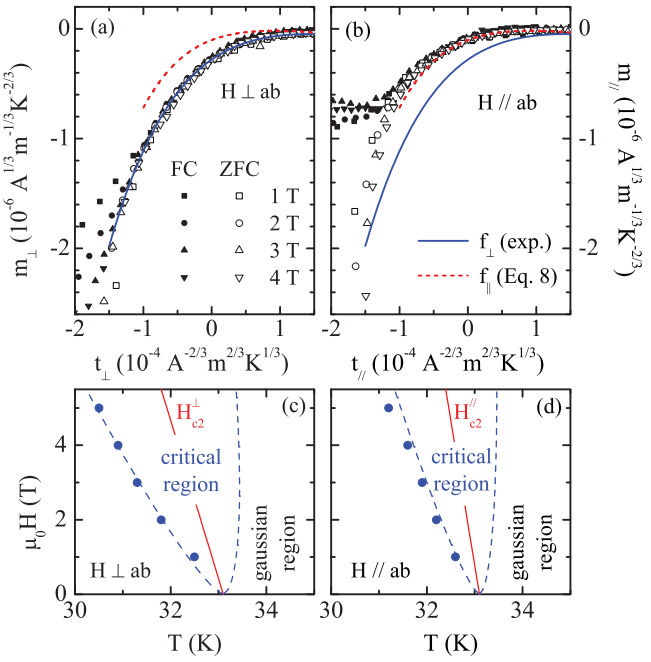

FIG. 4. (Color online) 3D-GL scaling of the magnetization in the critical region for $H \perp ab$ (a) and $H \parallel ab$ (b). The solid blue line is the *experimental* scaling function for $H \perp ab$, while the dashed red one corresponds to $H \parallel ab$ and was calculated from $f_{\perp}$ through Eq. (11). (c) and (d) H-T phase diagrams for $H \perp ab$ and, respectively, $H \parallel ab$. The corresponding $H_{c2}(T)$ lines were obtained from the superconducting parameters obtained in the analysis. The symbols are the lower bound of the reversible region, and the dashed lines the limits of the critical region according to Eqs. (7) and (8).

IV. CONCLUSIONS

The present experimental results and analysis represent a solid evidence that the precursor diamagnetism and the magnetization in the critical region around T_c in $Ba_{1-x}K_xFe_2As_2$ may be consistently explained at a phenomenological level in terms of a conventional GL approach for 3D anisotropic superconductors. This provides a strong constraint for any microscopic theory for the superconductivity in iron pnictides, and may have implications in systems like the HTSC, with similar superconducting parameters and possibly a similar mechanism for their superconductivity. It would be interesting

to extend these measurements to other iron pnictides with other type of substitution and doping levels, and also in larger samples to confirm whether the onset of the precursor diamagnetism is close to 1.7 T_c, as proposed by the total-energy cutoff scenario.

ACKNOWLEDGMENTS

This work was supported by the Spanish MICINN and ERDF (grant no. FIS2010-19807), and by the Xunta de Galicia (grants no. 2010/XA043 and 10TMT206012PR). SSS and ADA acknowledge support from the CNPq and FAPERJ.

*j.mosqueira@usc.es

[1] Y. Kamihara, T. Watanabe, M. Hitano, and H. Hosono, J. Am. Chem. Soc. **130**, 3296 (2008).

[2] For some reviews see, e.g., J. Paglione and R. L. Greene, Nature Phys. **6**, 645 (2010); K. Ishida, Y. Nakai, and H. Hosono, J. Phys. Soc. Jpn. **78**, 062001 (2009); D. C. Johnston, Adv. Phys. **59**, 803 (2010).

[3] J. P. Gollub, M. R. Beasley, R. S. Newbower, and M. Tinkham, Phys. Rev. Lett. **22**, 1288 (1969); J. P. Gollub, M. R. Beasley, R. Callarotti, and M. Tinkham, Phys. Rev. B **7**, 3039 (1973).

[4] For an introductory review see, e.g., M. Tinkham, *Introduction to Superconductivity* (McGraw-Hill, New York, 1996), Chap. 8.

[5] W. C. Lee, R. A. Klemm, and D. C. Johnston, Phys. Rev. Lett. **63**, 1012 (1989).

[6] For a review see, e.g., F. Vidal and M. V. Ramallo, in *The Gap Symmetry and Fluctuations in High T_c Superconductors*, edited by J. Bok, G. Detscher, D. Pavuna, and S. A. Wolf (Plenum, London, 1998), p. 477.

[7] C. Carballeira, J. Mosqueira, A. Revcolevschi, and F. Vidal, Phys. Rev. Lett. **84**, 3157 (2000).

[8] The few works on the fluctuation diamagnetism in iron pnictides published until now focus only on the critical region below T_c. See, e.g., S. Salem-Sugui Jr., L. Ghivelder, A. D. Alvarenga, J. L. Pimentel Jr., H. Luo, Z. Wang, and H-H. Wen, Phys. Rev. B **80**, 014518 (2009); C. Choi, S. Hyun Kim, K-Y. Choi, M-H. Jung, S.-I. Lee, X. F. Wang, X. H. Chen, and X. L. Wang, Supercond. Sci. Technol. **22**, 105016 (2009).

[9] See, e.g., E. Bernardi, A. Lascialfari, A. Rigamonti, L. Romanó, M. Scavini, and C. Oliva, Phys. Rev. B **81**, 064502 (2010), and references therein. Note, however, that conventional GL approaches were shown to be in excellent quantitative agreement with the precursor diamagnetism of high quality samples of several HTSC families, see, e.g.,; J. Mosqueira, C. Carballeira, M. V. Ramallo, C. Torrón, J. A. Veira, and F. Vidal, Europhys. Lett. **53**, 632 (2001); L. Cabo, J. Mosqueira, and F. Vidal, Phys. Rev. Lett. **98**, 119701 (2007); J. Mosqueira, L. Cabo, and F. Vidal, Phys. Rev. B **76**, 064521 (2007); J. Mosqueira and F. Vidal, *ibid.* **77**, 052507 (2008). Also, some of the anomalies observed in the precursor diamagnetism may be easily explained in terms of T_c inhomogeneities, which in the case of doped HTSC could even have an *intrinsic* origin, see, e.g.,; L. Cabo, F. Soto, M. Ruibal, J. Mosqueira, and F. Vidal, *ibid.* **73**, 184520 (2006); J. Mosqueira, L. Cabo, and F. Vidal, *ibid.* **80**, 214527 (2009).

[10] See, e.g., T. Kondo *et al.*, Nature (London) **457**, 297 (2009), and references therein.

[11] J. M. Murray and Z. Tešanović, Phys. Rev. Lett. **105**, 037006 (2010).

[12] F. Soto, H. Berger, L. Cabo, C. Carballeira, J. Mosqueira, D. Pavuna, and F. Vidal, Phys. Rev. B **75**, 094509 (2007).

[13] H. Luo, Z. Wang, H. Yang, P. Cheng, X. Zhu, and H-H. Wen, Supercond. Sci. Technol. **21**, 125014 (2008).

[14] In the presence of a crystal misalignment ($\theta_\perp$ or $\theta_\parallel$ when measuring with $H \perp ab$ or $H \parallel ab$, respectively) the ratio $M_\perp/M_\parallel$ is given by $\gamma_{\rm eff}^2 = (\gamma^2 \cos^2\theta_\perp + \sin^2\theta_\perp)/(\gamma^2 \sin^2\theta_\parallel + \cos^2\theta_\parallel)$ according to the 3D-AGL approach [see also J. Mosqueira, M. V. Ramallo, A. Revcolevschi, C. Torrón, and F. Vidal, Phys. Rev. B **59**, 4394 (1999)]. By using $\theta_\perp \sim 5^\circ$, $\theta_\parallel \sim 0.1^\circ$, and $\gamma \sim 1.8$, the resulting $\gamma_{\rm eff}$ value is only $\sim 0.5\%$ away from γ.

[15] R. A. Klemm and J. R. Clem, Phys. Rev. B **21**, 1868 (1980).

[16] G. Blatter, V. B. Geshkenbein, and A. I. Larkin, Phys. Rev. Lett. **68**, 875 (1992).

[17] Z. Hao and J. R. Clem, Phys. Rev. B **46**, 5853 (1992).

[18] J. Mosqueira, C. Carballeira, and F. Vidal, Phys. Rev. Lett. **87**, 167009 (2001); see also, J. Mosqueira, C. Carballeira, S. R. Currás, M. T. González, M. V. Ramallo, M. Ruibal, C. Torrón, and F. Vidal, J. Phys. Condens. Matter **15**, 3283 (2003).

[19] F. Vidal, C. Carballeira, S. R. Currás, J. Mosqueira, M. V. Ramallo, J. A. Veira, and J. Vina, Europhys. Lett. **59**, 754 (2002).

[20] H. Schmidt, Z. Phys. **216**, 336 (1968); A. Schmid, Phys. Rev. **180**, 527 (1969).

[21] According to Eq. (4), the sample volume needed to determine the onset of the precursor diamagnetism with a 10% accuracy in reduced temperature is $V \sim 50\phi_0^2 \delta m / k_B T_c \mu_0 H \gamma \xi_{ab}(0)$, where $\delta m \sim 10^{-8}$ emu is our experimental resolution in magnetic moment. In the present case this leads to $V \approx 2\ {\rm mm}^3$ (~ 30 times larger than in our crystal). In practice, the uncertainty associated to the background determination leads to an even more restrictive condition.

[22] F. Soto, C. Carballeira, J. Mosqueira, M. V. Ramallo, M. Ruibal, J. A. Veira, and F. Vidal, Phys. Rev. B **70**, 060501(R) (2004).

[23] U. Welp, R. Xie, A. E. Koshelev, W. K. Kwok, H. Q. Luo, Z. S. Wang, G. Mu, and H. H. Wen, Phys. Rev. B **79**, 094505 (2009); see also V. G. Kogan, *ibid.* **80**, 214532 (2009), and references therein.

[24] R. Ikeda, T. Ohmi, and T. Tsuneto, J. Phys. Soc. Jpn. **58**, 1377 (1989); **59**, 1397 (1990); D. H. Kim, K. E. Gray, and M. D. Trochet, Phys. Rev. B **45**, 10801 (1992).

[25] S. Ullah and A. T. Dorsey, Phys. Rev. Lett. **65**, 2066 (1990); Phys. Rev. B **44**, 262 (1991).

[26] J. Zaanen, Phys. Rev. B **80**, 212502 (2009).